15

The stochastic matched filter and its applications to detection and de-noising

Philippe Courmontagne
ISEN Toulon - IM2NP
FRANCE

1. Introduction

In several domains of signal processing, such as detection or de-noising, it may be interesting to provide a second-moment characterization of a noise-corrupted signal in terms of uncorrelated random variables. Doing so, the noisy data could be described by its expansion into a weighted sum of known vectors by uncorrelated random variables. Depending on the choice of the basis vectors, some random variables are carrying more signal of interest informations than noise ones. This is the case, for example, when a signal disturbed by a white noise is expanded using the Karhunen-Loève expansion (Karhunen, 1946; Loève, 1955). In these conditions, it is possible either to approximate the signal of interest considering, for the reconstruction, only its associated random variables, or to detect a signal in a noisy environment with an analysis of the random variable power. The purpose of this chapter is to present such an expansion, available for both the additive and multiplicative noise cases, and its application to detection and de-noising. This noisy random signal expansion is known as the stochastic matched filter (Cavassilas, 1991), where the basis vectors are chosen so as to maximize the signal to noise ratio after processing.
At first, we recall some general considerations on a random 1-D discrete-time signal expansion in section 2. In particular, we study the approximation error and the second order statistics of the signal approximation. Then, in section 3, we describe the stochastic matched filter theory for 1-D discrete-time signals and its extension to 2-D discrete-space signals. We finish this section with a study on two different noise cases: the white noise case and the speckle noise case. In the next section, we present the stochastic matched filter in a de-noising context and we briefly discuss the estimator bias. Then, the de-noising being performed by a limitation to order Q of the noisy data expansion, we propose to determine this truncature order using a mean square error criterion. Experimental results on synthetic and real data are given and discussed to evaluate the performances of such an approach. In section 5, we describe the stochastic matched filter in a detection context and we confront the proposed method with signals resulting from underwater acoustics. Finally, some concluding remarks are given in section 6.

2. Random signal expansion

2.1 1-D discrete-time signals

Let $\mathbf{S}$ be a zero mean, stationary, discrete-time random signal, made of M successive samples and let $\{s_1, s_2, \ldots, s_M\}$ be a zero mean, uncorrelated random variable sequence, i.e.:

$$E\{s_n s_m\} = E\left\{s_m^2\right\}\delta_{n,m}, \tag{1}$$

where $\delta_{n,m}$ denotes the Kronecker symbol.
It is possible to expand signal $\mathbf{S}$ into series of the form:

$$\mathbf{S} = \sum_{m=1}^{M} s_m \mathbf{\Psi_m}, \tag{2}$$

where $\{\mathbf{\Psi_m}\}_{m=1\ldots M}$ corresponds to a M-dimensional deterministic basis. Vectors $\mathbf{\Psi_m}$ are linked to the choice of random variables sequence $\{s_m\}$, so there are many decompositions (2).
These vectors are determined by considering the mathematical expectation of the product of s_m with the random signal $\mathbf{S}$. It comes:

$$\mathbf{\Psi_m} = \frac{1}{E\left\{s_m^2\right\}} E\{s_m \mathbf{S}\}. \tag{3}$$

Classically and using a M-dimensional deterministic basis $\{\mathbf{\Phi_m}\}_{m=1\ldots M}$, the random variables s_m can be expressed by the following relation:

$$s_m = \mathbf{S}^T \mathbf{\Phi_m}. \tag{4}$$

The determination of these random variables depends on the choice of the basis $\{\mathbf{\Phi_m}\}_{m=1\ldots M}$.
We will use a basis, which provides the uncorrelation of the random variables. Using relations (1) and (4), we can show that the uncorrelation is ensured, when vectors $\mathbf{\Phi_m}$ are solution of the following quadratic form:

$$\mathbf{\Phi_m}^T \mathbf{\Gamma_{SS}} \mathbf{\Phi_n} = E\left\{s_m^2\right\}\delta_{n,m}, \tag{5}$$

where $\mathbf{\Gamma_{SS}}$ represents the signal covariance.
There is an infinity of sets of vectors obtained by solving the previous equation. Assuming that a basis $\{\mathbf{\Phi_m}\}_{m=1\ldots M}$ is chosen, we can find random variables using relation (4). Taking into account relations (3) and (4), we obtain as new expression for $\mathbf{\Psi_m}$:

$$\mathbf{\Psi_m} = \frac{1}{E\left\{s_m^2\right\}} \mathbf{\Gamma_{SS}} \mathbf{\Phi_m}. \tag{6}$$

Furthermore, using relations (5) and (6), we can show that vectors $\mathbf{\Psi_m}$ and $\mathbf{\Phi_m}$ are linked by the following bi-orthogonality relation:

$$\mathbf{\Phi_m}^T \mathbf{\Psi_n} = \delta_{n,m}. \tag{7}$$

2.2 Approximation error

When the discrete sum, describing the signal expansion (relation (2)), is reduced to Q random variables s_m, only an approximation $\widetilde{\mathbf{S}}_{\mathbf{Q}}$ of the signal is obtained:

$$\widetilde{\mathbf{S}}_{\mathbf{Q}} = \sum_{m=1}^{Q} s_m \mathbf{\Psi_m}. \tag{8}$$

To evaluate the error induced by the restitution, let us consider the mean square error ϵ between signal $\mathbf{S}$ and its approximation $\widetilde{\mathbf{S}}_{\mathbf{Q}}$:

$$\epsilon = E\left\{ \left\| \mathbf{S} - \widetilde{\mathbf{S}}_{\mathbf{Q}} \right\|^2 \right\}, \tag{9}$$

where $\|.\|$ denotes the classical Euclidean norm.
Considering the signal variance σ_S^2, it can be easily shown that:

$$\epsilon = \sigma_S^2 - \sum_{m=1}^{Q} E\left\{ s_m^2 \right\} \|\mathbf{\Psi_m}\|^2, \tag{10}$$

which corresponds to:

$$\epsilon = \sigma_S^2 - \sum_{m=1}^{Q} \frac{\mathbf{\Phi_m}^T \mathbf{\Gamma_{SS}}^2 \mathbf{\Phi_m}}{\mathbf{\Phi_m}^T \mathbf{\Gamma_{SS}} \mathbf{\Phi_m}}. \tag{11}$$

When we consider the whole s_m sequence (i.e. Q equal to M), the approximation error ϵ is weak, and coefficients given by the quadratic form ratio:

$$\frac{\mathbf{\Phi_m}^T \mathbf{\Gamma_{SS}}^2 \mathbf{\Phi_m}}{\mathbf{\Phi_m}^T \mathbf{\Gamma_{SS}} \mathbf{\Phi_m}}$$

are carrying the signal power.

2.3 Second order statistics

The purpose of this section is the determination of the $\widetilde{\mathbf{S}}_{\mathbf{Q}}$ autocorrelation and spectral power density. Let $\mathbf{\Gamma}_{\widetilde{\mathbf{S}}_{\mathbf{Q}}\widetilde{\mathbf{S}}_{\mathbf{Q}}}$ be the $\widetilde{S}_Q$ autocorrelation, we have:

$$\Gamma_{\widetilde{S}_Q\widetilde{S}_Q}[p] = E\left\{ \widetilde{S}_Q[q]\widetilde{S}_Q^*[p-q] \right\}. \tag{12}$$

Taking into account relation (8) and the uncorrelation of random variables s_m, it comes:

$$\Gamma_{\widetilde{S}_Q\widetilde{S}_Q}[p] = \sum_{m=1}^{Q} E\left\{ s_m^2 \right\} \Psi_m[q]\Psi_m^*[p-q], \tag{13}$$

which leads to, summing all elements of the previous relation:

$$\sum_{q=1}^{M} \Gamma_{\widetilde{S}_Q\widetilde{S}_Q}[p] = \sum_{q=1}^{M} \sum_{m=1}^{Q} E\left\{ s_m^2 \right\} \Psi_m[q]\Psi_m^*[p-q]. \tag{14}$$

So, we have:

$$\Gamma_{\widetilde{S}_Q\widetilde{S}_Q}[p] = \frac{1}{M}\sum_{m=1}^{Q} E\left\{s_m^2\right\}\sum_{q=1}^{M}\Psi_m[q]\Psi_m^*[p-q], \tag{15}$$

which corresponds to:

$$\Gamma_{\widetilde{S}_Q\widetilde{S}_Q}[p] = \frac{1}{M}\sum_{m=1}^{Q} E\left\{s_m^2\right\}\Gamma_{\Psi_m\Psi_m}[p]. \tag{16}$$

In these conditions, the $\widetilde{\mathbf{S}}_\mathbf{Q}$ spectral power density is equal to:

$$\gamma_{\widetilde{S}_Q\widetilde{S}_Q}(\nu) = \frac{1}{M}\sum_{m=1}^{Q} E\left\{s_m^2\right\}\gamma_{\Psi_m\Psi_m}(\nu). \tag{17}$$

3. The Stochastic Matched Filter expansion

Detecting or de-noising a signal of interest **S**, corrupted by an additive or multiplicative noise **N** is a usual signal processing problem. We can find in the literature several processing methods for solving this problem. One of them is based on a stochastic extension of the matched filter notion (Cavassilas, 1991; Chaillan et al., 2007; 2005). The signal of interest pattern is never perfectly known, so it is replaced by a random signal allowing a new formulation of the signal to noise ratio. The optimization of this ratio leads to design a bench of filters and regrouping them strongly increases the signal to noise ratio.

3.1 1-D discrete-time signals: signal-independent additive noise case

Let us consider a noise-corrupted signal **Z**, made of M successive samples and corresponding to the superposition of a signal of interest **S** with a colored noise **N**. If we consider the signal and noise variances, σ_S^2 and σ_N^2, we have:

$$\mathbf{Z} = \sigma_S\mathbf{S_0} + \sigma_N\mathbf{N_0}, \tag{18}$$

with $E\left\{\mathbf{S_0}^2\right\} = 1$ and $E\left\{\mathbf{N_0}^2\right\} = 1$. In the previous relation, reduced signals $\mathbf{S_0}$ and $\mathbf{N_0}$ are assumed to be independent, stationary and with zero-mean.
It is possible to expand noise-corrupted signal **Z** into a weighted sum of known vectors $\mathbf{\Psi_m}$ by uncorrelated random variables z_m, as described in relation (2). These uncorrelated random variables are determined using the scalar product between noise-corrupted signal **Z** and deterministic vectors $\mathbf{\Phi_m}$ (see relation (4)). In order to determine basis $\{\mathbf{\Phi_m}\}_{m=1\ldots M}$, let us describe the matched filter theory. If we consider a discrete-time, stationary, known input signal **s**, made of M successive samples, corrupted by an ergodic reduced noise $\mathbf{N_0}$, the matched filter theory consists of finding an impulse response $\mathbf{\Phi}$, which optimizes the signal to noise ratio ρ. Defined as the ratio of the square of signal amplitude to the square of noise amplitude, ρ is given by:

$$\rho = \frac{|\mathbf{s}^T\mathbf{\Phi}|^2}{E\left\{|\mathbf{N_0}^T\mathbf{\Phi}|^2\right\}}. \tag{19}$$

When the signal is not deterministic, i.e. a random signal $\mathbf{S_0}$, this ratio becomes (Cavassilas, 1991):

$$\rho = \frac{E\left\{|\mathbf{S_0}^T\mathbf{\Phi}|^2\right\}}{E\left\{|\mathbf{N_0}^T\mathbf{\Phi}|^2\right\}}, \tag{20}$$

which leads to:

$$\rho = \frac{\mathbf{\Phi}^T \mathbf{\Gamma_{S_0S_0}} \mathbf{\Phi}}{\mathbf{\Phi}^T \mathbf{\Gamma_{N_0N_0}} \mathbf{\Phi}}, \tag{21}$$

where $\mathbf{\Gamma_{S_0S_0}}$ and $\mathbf{\Gamma_{N_0N_0}}$ represent signal and noise reduced covariances respectively.
Relation (21) corresponds to the ratio of two quadratic forms. It is a Rayleigh quotient. For this reason, the signal to noise ratio ρ is maximized when the impulse response $\mathbf{\Phi}$ corresponds to the eigenvector $\mathbf{\Phi_1}$ associated to the greatest eigenvalue λ_1 of the following generalized eigenvalue problem:

$$\mathbf{\Gamma_{S_0S_0}} \mathbf{\Phi_m} = \lambda_m \mathbf{\Gamma_{N_0N_0}} \mathbf{\Phi_m}. \tag{22}$$

Let us consider the signal and noise expansions, we have:

$$\begin{cases} \mathbf{S_0} = \sum_{m=1}^{M} s_m \mathbf{\Psi_m} \\ \mathbf{N_0} = \sum_{m=1}^{M} \eta_m \mathbf{\Psi_m} \end{cases}, \tag{23}$$

where the random variables defined by:

$$\begin{cases} s_m = \mathbf{\Phi_m}^T \mathbf{S_0} \\ \eta_m = \mathbf{\Phi_m}^T \mathbf{N_0} \end{cases} \tag{24}$$

are not correlated:

$$\begin{cases} \mathbf{\Phi_m}^T \mathbf{\Gamma_{S_0S_0}} \mathbf{\Phi_n} = E\left\{s_m^2\right\} \delta_{n,m} \\ \mathbf{\Phi_m}^T \mathbf{\Gamma_{N_0N_0}} \mathbf{\Phi_n} = E\left\{\eta_m^2\right\} \delta_{n,m} \end{cases}. \tag{25}$$

After a normalization step; it is possible to rewrite relations (25) as follows:

$$\begin{cases} \mathbf{\Phi_m}^T \mathbf{\Gamma_{S_0S_0}} \mathbf{\Phi_n} = \dfrac{E\left\{s_m^2\right\}}{E\left\{\eta_m^2\right\}} \delta_{n,m} \\ \mathbf{\Phi_m}^T \mathbf{\Gamma_{N_0N_0}} \mathbf{\Phi_n} = \delta_{n,m} \end{cases}. \tag{26}$$

Let $\mathbf{P}$ be a matrix made up of column vectors $\mathbf{\Phi_m}$, i.e.:

$$\mathbf{P} = \left(\mathbf{\Phi_1}, \mathbf{\Phi_2}, \ldots, \mathbf{\Phi_M}\right). \tag{27}$$

In these conditions, it comes:

$$\mathbf{P}^T \mathbf{\Gamma_{N_0N_0}} \mathbf{P} = \mathbf{I}, \tag{28}$$

where $\mathbf{I}$ corresponds to the identity matrix.
This leads to:

$$\begin{aligned} & \left(\mathbf{P}^T \mathbf{\Gamma_{N_0N_0}} \mathbf{P}\right)^{-1} = \mathbf{I} \\ \Leftrightarrow \quad & \mathbf{P}^{-1} \mathbf{\Gamma_{N_0N_0}}^{-1} \mathbf{P}^{-T} = \mathbf{I} \\ \Leftrightarrow \quad & \mathbf{P}^T = \mathbf{P}^{-1} \mathbf{\Gamma_{N_0N_0}}^{-1}. \end{aligned} \tag{29}$$

Let $\mathbf{D}$ be the following diagonal matrix:

$$\mathbf{D} = \begin{pmatrix} E\left\{s_1^2\right\}/E\left\{\eta_1^2\right\} & 0 & \ldots & \ldots & 0 \\ 0 & E\left\{s_2^2\right\}/E\left\{\eta_2^2\right\} & 0 & \ldots & 0 \\ \vdots & \ddots & \ddots & \ddots & \vdots \\ 0 & \ldots & 0 & E\left\{s_{M-1}^2\right\}/E\left\{\eta_{M-1}^2\right\} & 0 \\ 0 & \ldots & \ldots & 0 & E\left\{s_M^2\right\}/E\left\{\eta_M^2\right\} \end{pmatrix}. \tag{30}$$

It comes:

$$\mathbf{P}^T \mathbf{\Gamma}_{\mathbf{S_0 S_0}} \mathbf{P} = \mathbf{D}, \tag{31}$$

which corresponds to, taking into account relation (29):

$$\begin{aligned} & \mathbf{P}^{-1} \mathbf{\Gamma}_{\mathbf{N_0 N_0}}{}^{-1} \mathbf{\Gamma}_{\mathbf{S_0 S_0}} \mathbf{P} = \mathbf{D} \\ \Leftrightarrow \quad & \mathbf{\Gamma}_{\mathbf{N_0 N_0}}{}^{-1} \mathbf{\Gamma}_{\mathbf{S_0 S_0}} \mathbf{P} = \mathbf{P D} \\ \Leftrightarrow \quad & \mathbf{\Gamma}_{\mathbf{S_0 S_0}} \mathbf{P} = \mathbf{\Gamma}_{\mathbf{N_0 N_0}} \mathbf{P D}, \end{aligned} \tag{32}$$

which leads to:

$$\mathbf{\Gamma}_{\mathbf{S_0 S_0}} \mathbf{\Phi_m} = \frac{E\left\{s_m^2\right\}}{E\left\{\eta_m^2\right\}} \mathbf{\Gamma}_{\mathbf{N_0 N_0}} \mathbf{\Phi_m}. \tag{33}$$

This last equation shows, on the one hand, that λ_m equals $E\left\{s_m^2\right\} / E\left\{\eta_m^2\right\}$ and, on the other hand, that the only basis $\left\{\mathbf{\Phi_m}\right\}_{m=1\ldots M}$ allowing the simultaneous uncorrelation of the random variables coming from the signal and the noise is made up of vectors $\mathbf{\Phi_m}$ solution of the generalized eigenvalue problem (22).
We have $E\left\{\eta_m^2\right\} = 1$ and $E\left\{s_m^2\right\} = \lambda_m$ when the eigenvectors $\mathbf{\Phi_m}$ are normalized as follows:

$$\mathbf{\Phi_m}^T \mathbf{\Gamma}_{\mathbf{N_0 N_0}} \mathbf{\Phi_m} = 1, \tag{34}$$

In these conditions and considering relation (6), the deterministic vectors $\mathbf{\Psi_m}$ of the noise-corrupted signal expansion are given by:

$$\mathbf{\Psi_m} = \mathbf{\Gamma}_{\mathbf{N_0 N_0}} \mathbf{\Phi_m}. \tag{35}$$

In this context, the noise-corrupted signal expansion is expressed as follows:

$$\mathbf{Z} = \sum_{m=1}^{M} (\sigma_S s_m + \sigma_N \eta_m) \mathbf{\Psi_m}, \tag{36}$$

so that, the quadratic moment of the mth coefficient z_m of the noise-corrupted signal expansion is given by:

$$E\left\{z_m^2\right\} = E\left\{(\sigma_S s_m + \sigma_N \eta_m)^2\right\}, \tag{37}$$

which corresponds to:

$$\sigma_S^2 \lambda_m + \sigma_N^2 + \sigma_S \sigma_N \mathbf{\Phi_m}^T \left(\mathbf{\Gamma}_{\mathbf{S_0 N_0}} + \mathbf{\Gamma}_{\mathbf{N_0 S_0}}\right) \mathbf{\Phi_m} \tag{38}$$

Signal and noise being independent and one of them at least being zero mean, we can assume that the cross-correlation matrices, $\mathbf{\Gamma}_{\mathbf{S_0 N_0}}$ and $\mathbf{\Gamma}_{\mathbf{N_0 S_0}}$, are weak. In this condition, the signal to noise ratio ρ_m of component z_m corresponds to the native signal to noise ratio times eigenvalue λ_m:

$$\rho_m = \frac{\sigma_S^2}{\sigma_N^2} \lambda_m. \tag{39}$$

So, an approximation $\widetilde{\mathbf{S}}_{\mathbf{Q}}$ of the signal of interest (the filtered noise-corrupted signal) can be built by keeping only those components associated to eigenvalues greater than a certain threshold. In any case this threshold is greater than one.

3.2 Extension to 2-D discrete-space signals

We consider now a $M \times M$ pixels two-dimensional noise-corrupted signal, $\mathbf{Z}$, which corresponds to a signal of interest $\mathbf{S}$ disturbed by a noise $\mathbf{N}$. The two-dimensional extension of the theory developed in the previous section gives:

$$\mathbf{Z} = \sum_{m=1}^{M^2} z_m \mathbf{\Psi_m}, \tag{40}$$

where $\{\mathbf{\Psi_m}\}_{m=1...M^2}$ is a M^2-dimensional basis of $M \times M$ matrices.
Random variables z_m are determined, using a M^2-dimensional basis $\{\mathbf{\Phi_m}\}_{m=1...M^2}$ of $M \times M$ matrices, as follows:

$$z_m = \sum_{p,q=1}^{M} Z[p,q]\Phi_m[p,q]. \tag{41}$$

These random variables will be not correlated, if matrices $\mathbf{\Phi_m}$ are solution of the two-dimensional extension of the generalized eigenvalue problem (22):

$$\sum_{p_1,q_1=1}^{M} \Gamma_{S_0S_0}[p_1 - p_2, q_1 - q_2]\Phi_m[p_1,q_1] = \lambda_n \sum_{p_1,q_1=1}^{M} \Gamma_{N_0N_0}[p_1 - p_2, q_1 - q_2]\Phi_m[p_1,q_1], \tag{42}$$

for all $p_2, q_2 = 1, \ldots, M$.
Assuming that $\mathbf{\Phi_m}$ are normalized as follows:

$$\sum_{p_1,p_2,q_1,q_2=1}^{M} \Gamma_{N_0N_0}[p_1 - p_2, q_1 - q_2]\Phi_m[p_1,q_1]\Phi_m[p_2,q_2] = 1, \tag{43}$$

the basis $\{\mathbf{\Psi_m}\}_{m=1...M^2}$ derives from:

$$\Psi_m[p_1,q_1] = \sum_{p_2,q_2=1}^{M} \Gamma_{N_0N_0}[p_1 - p_2, q_1 - q_2]\Phi_m[p_2,q_2]. \tag{44}$$

As for the 1-D discrete-time signals case, using such an expansion leads to a signal to noise ratio of component z_m equal to the native signal to noise ratio times eigenvalue λ_m (see relation (39)). So, all $\mathbf{\Phi_m}$ associated to eigenvalues λ_m greater than a certain level - in any case greater than one - can contribute to an improvement of the signal to noise ratio.

3.3 The white noise case

When $\mathbf{N}$ corresponds to a white noise, its reduced covariance is:

$$\Gamma_{N_0N_0}[p-q] = \delta[p-q]. \tag{45}$$

Thus, the generalized eigenvalue problem (22) leading to the determination of vectors $\mathbf{\Phi_m}$ and associated eigenvalues is reduced to:

$$\mathbf{\Gamma_{S_0S_0}\Phi_m} = \lambda_m \mathbf{\Phi_m}. \tag{46}$$

In this context, we can show that basis vectors $\mathbf{\Psi_m}$ and $\mathbf{\Phi_m}$ are equal. Thus, in the particular case of a white noise, the stochastic matched filter theory is identical to the Karhunen-Loève expansion (Karhunen, 1946; Loève, 1955):

$$\mathbf{Z} = \sum_{m=1}^{M} z_m \mathbf{\Phi_m}. \quad (47)$$

One can show that when the signal covariance is described by a decreasing exponential function ($\Gamma_{S_0S_0}(t_1, t_2) = e^{-\alpha|t_1-t_2|}$, with $\alpha \in \mathbb{R}^{+*}$), basis $\{\mathbf{\Phi_m}\}_{m=1...M}$ corresponds to the Fourier basis (Vann Trees, 1968), so that the Fourier expansion is a particular case of the Karhunen-Loève expansion, which is a particular case of the stochastic matched filter expansion.

3.4 The speckle noise case

Some airborne SAR (Synthetic Aperture Radar) imaging devices randomly generate their own corrupting signal, called the speckle noise, generally described as a multiplicative noise (Tur et al., 1982). This is due to the complexity of the techniques developed to get the best resolution of the ground. Given experimental data accuracy and quality, these systems have been used in sonars (SAS imaging device), with similar characteristics.
Under these conditions, we cannot anymore consider the noise-corrupted signal as described in (18), so its expression becomes:

$$\mathbf{Z} = \mathbf{S} .* \mathbf{N}, \quad (48)$$

where $.*$ denotes the term by term product.
In order to fall down in a known context, let consider the Kuan approach (Kuan et al., 1985). Assuming that the multiplicative noise presents a stationary mean ($\bar{N} = E\{\mathbf{N}\}$), we can define the following normalized observation:

$$\mathbf{Z_{norm}} = \mathbf{Z}/\bar{N}. \quad (49)$$

In this condition, we can represent (49) in terms of signal plus signal-dependent additive noise:

$$\mathbf{Z_{norm}} = \mathbf{S} + \left(\frac{\mathbf{N} - \bar{N}}{\bar{N}}\right) .* \mathbf{S}. \quad (50)$$

Let $\mathbf{N_a}$ be this signal-dependent additive colored noise:

$$\mathbf{N_a} = (\mathbf{N}/\bar{N} - 1) .* \mathbf{S}. \quad (51)$$

Under these conditions, the mean quadratic value of the mth component z_m of the normalized observation expansion is:

$$E\left\{z_m^2\right\} = \sigma_S^2 \lambda_n + \sigma_{N_a}^2 + \sigma_S \sigma_{N_a} \mathbf{\Phi_m}^T \left(\mathbf{\Gamma_{S_0 N_{a_0}}} + \mathbf{\Gamma_{N_{a_0} S_0}}\right) \mathbf{\Phi_m}, \quad (52)$$

where $\mathbf{N_{a_0}}$ corresponds to the reduced noise $\mathbf{N_a}$.
Consequently, the signal to noise ratio ρ_m becomes:

$$\rho_m = \frac{\sigma_S^2 \lambda_m}{\sigma_{N_a}^2 + \sigma_S \sigma_{N_a} \mathbf{\Phi_m}^T \left(\mathbf{\Gamma_{S_0 N_{a_0}}} + \mathbf{\Gamma_{N_{a_0} S_0}}\right) \mathbf{\Phi_m}}. \quad (53)$$

As $\mathbf{S_0}$ and $(\mathbf{N}/\bar{N}-1)$ are independent, it comes:

$$\Gamma_{S_0 N_{a_0}}[p_1,p_2,q_1,q_2] = E\left\{S_0[p_1,q_1]N_{a_0}[p_2,q_2]\right\}, \tag{54}$$

which is equal to:

$$\frac{1}{\sigma_{N_a}} E\left\{S_0[p_1,q_1]S[p_2,q_2]\right\} \underbrace{\left(\frac{E\{N[p_2,q_2]\}}{\bar{N}} - 1\right)}_{=0} = 0. \tag{55}$$

So that, the cross-correlation matrices between signal $\mathbf{S_0}$ and signal-dependent noise $\mathbf{N_{a_0}}$ vanishes. For this reason, signal to noise ratio in a context of multiplicative noise like the speckle noise, expanded into the stochastic matched filter basis has the same expression than in the case of an additive noise.

4. The Stochastic Matched Filter in a de-noising context

In this section, we present the stochastic matched filtering in a de-noising context for 1-D discrete time signals. The given results can easily be extended to higher dimensions.

4.1 Bias estimator

Let $\mathbf{Z}$ be a M-dimensional noise corrupted observed signal. The use of the stochastic matched filter as a restoring process is based on the decomposition of this observation, into a random variable finite sequence z_m on the $\{\mathbf{\Psi_m}\}_{m=1\ldots M}$ basis. An approximation $\widetilde{\mathbf{S}}_\mathbf{Q}$ is obtained with the z_m coefficients and the Q basis vectors $\mathbf{\Psi_m}$, with Q lower than M:

$$\widetilde{\mathbf{S}}_\mathbf{Q} = \sum_{m=1}^{Q} z_m \mathbf{\Psi_m}. \tag{56}$$

If we examine the M-dimensional vector $\mathbf{E}\left\{\widetilde{\mathbf{S}}_\mathbf{Q}\right\}$, we have:

$$\begin{aligned} \mathbf{E}\left\{\widetilde{\mathbf{S}}_\mathbf{Q}\right\} &= E\left\{\sum_{m=1}^{Q} \mathbf{\Psi_m} z_m\right\} \\ &= \sum_{m=1}^{Q} \mathbf{\Psi_m}\mathbf{\Phi_m^T}\mathbf{E}\left\{\mathbf{Z}\right\} \end{aligned} \tag{57}$$

Using the definition of noise-corrupted signal $\mathbf{Z}$, it comes:

$$\mathbf{E}\left\{\widetilde{\mathbf{S}}_\mathbf{Q}\right\} = \sum_{m=1}^{Q} \mathbf{\Psi_m}\mathbf{\Phi_m^T}\left(\mathbf{E}\left\{\mathbf{S}\right\} + \mathbf{E}\left\{\mathbf{N}\right\}\right). \tag{58}$$

Under these conditions, the estimator bias $B_{\widetilde{S}_Q}$ can be expressed as follows:

$$\begin{aligned} B_{\widetilde{S}_Q} &= E\left\{\widetilde{\mathbf{S}}_\mathbf{Q} - \mathbf{S}\right\} \\ &= \left(\sum_{m=1}^{Q} \mathbf{\Psi_m}\mathbf{\Phi_m^T} - \mathbf{I}\right)\mathbf{E}\left\{\mathbf{S}\right\} + \sum_{m=1}^{Q} \mathbf{\Psi_m}\mathbf{\Phi_m^T}\mathbf{E}\left\{\mathbf{N}\right\}, \end{aligned} \tag{59}$$

where $\mathbf{I}$ denotes the $M \times M$ identity matrix.
Furthermore, if we consider the signal of interest expansion, we have:

$$\mathbf{S} = \left(\sum_{m=1}^{M} \mathbf{\Psi_m} \mathbf{\Phi_m^T} \right) \mathbf{S}, \tag{60}$$

so that, by identification, it comes:

$$\sum_{m=1}^{M} \mathbf{\Psi_m} \mathbf{\Phi_m^T} = \mathbf{I}. \tag{61}$$

In this condition, relation (59) can be rewritten as follows:

$$B_{\widetilde{S}_Q} = - \sum_{m=Q+1}^{M} \mathbf{\Psi_m} \mathbf{\Phi_m^T} \mathbf{E}\left\{\mathbf{S}\right\} + \sum_{m=1}^{Q} \mathbf{\Psi_m} \mathbf{\Phi_m^T} \mathbf{E}\left\{\mathbf{N}\right\}. \tag{62}$$

This last equation corresponds to the estimator bias when no assumption is made on the signal and noise mean values. In our case, signal and noise are both supposed zero-mean, so that the stochastic matched filter allows obtaining an unbiased estimation of the signal of interest.

4.2 De-noising using a mean square error minimization

4.2.1 Problem description

In many signal processing applications, it is necessary to estimate a signal of interest disturbed by an additive or multiplicative noise. We propose here to use the stochastic matched filtering technique as a de-noising process, such as the mean square error between the signal of interest and its approximation will be minimized.

4.2.2 Principle

In the general theory of stochastic matched filtering, Q is chosen so as the Q first eigenvalues, coming from the generalized eigenvalue problem, are greater than one, in order to enhance the m^{th} component of the observation. To improve this choice, let us consider the mean square error ϵ between the signal of interest $\mathbf{S}$ and its approximation $\widetilde{\mathbf{S}}_\mathbf{Q}$:

$$\epsilon = E\left\{ \left(\mathbf{S} - \widetilde{\mathbf{S}}_\mathbf{Q}\right)^T \left(\mathbf{S} - \widetilde{\mathbf{S}}_\mathbf{Q}\right) \right\}. \tag{63}$$

It is possible to show that this error, function of Q, can be written as:

$$\epsilon(Q) = \sigma_S^2 \left(1 - \sum_{m=1}^{Q} \lambda_n \left\| \mathbf{\Psi_m} \right\|^2 \right) + \sigma_N^2 \sum_{m=1}^{Q} \left\| \mathbf{\Psi_m} \right\|^2. \tag{64}$$

The integer Q is chosen so as to minimize the relation (64). It particularly verifies:

$$(\epsilon(Q) - \epsilon(Q-1)) < 0 \quad \& \quad (\epsilon(Q+1) - \epsilon(Q)) > 0,$$

let us explicit these two inequalities; on the one hand:

$$\epsilon(Q+1) - \epsilon(Q) = \left(\sigma_N^2 - \sigma_S^2 \lambda_{Q+1}\right) \left\| \mathbf{\Psi_{Q+1}} \right\|^2 > 0$$

and on the other hand:

$$\epsilon(Q) - \epsilon(Q-1) = \left(\sigma_N^2 - \sigma_S^2 \lambda_Q\right) \|\mathbf{\Psi_Q}\|^2 < 0.$$

Hence, integer Q verifies:

$$\sigma_S^2 \lambda_Q > \sigma_N^2 > \sigma_S^2 \lambda_{Q+1}.$$

The dimension of the basis $\{\mathbf{\Psi_m}\}_{m=1...Q}$, which minimizes the mean square error between the signal of interest and its approximation, is the number of eigenvalues λ_m verifying:

$$\frac{\sigma_S^2}{\sigma_N^2} \lambda_m > 1, \tag{65}$$

where $\frac{\sigma_S^2}{\sigma_N^2}$ is the signal to noise ratio before processing.

Consequently, if the observation has a high enough signal to noise ratio, many $\mathbf{\Psi_m}$ will be considered for the filtering (so that $\widetilde{\mathbf{S}}_\mathbf{Q}$ tends to be equal to $\mathbf{Z}$), and in the opposite case, only a few number will be chosen. In these conditions, this filtering technique applied to an observation $\mathbf{Z}$ with an initial signal to noise ratio $\left.\frac{S}{N}\right|_\mathbf{Z}$ substantially enhances the signal of interest perception. Indeed, after processing, the signal to noise ratio $\left.\frac{S}{N}\right|_{\widetilde{\mathbf{S}}_\mathbf{Q}}$ becomes:

$$\left.\frac{S}{N}\right|_{\widetilde{\mathbf{S}}_\mathbf{Q}} = \left.\frac{S}{N}\right|_\mathbf{Z} \frac{\sum\limits_{m=1}^{Q} \lambda_m \|\mathbf{\Psi_m}\|^2}{\sum\limits_{m=1}^{Q} \|\mathbf{\Psi_m}\|^2}. \tag{66}$$

4.2.3 The Stochastic Matched Filter

As described in a forthcoming section, the stochastic matched filtering method is applied using a sliding sub-window processing. Therefore, let consider a K-dimensional vector $\mathbf{Z_k}$ corresponding to the data extracted from a window centered on index k of the noisy data, i.e.:

$$\mathbf{Z_k}^T = \left\{ Z\left[k - \frac{K-1}{2}\right], \ldots, Z[k], \ldots, Z\left[k + \frac{K-1}{2}\right] \right\}. \tag{67}$$

This way, M sub-windows $\mathbf{Z_k}$ are extracted to process the whole observation, with $k = 1, \ldots, M$. Furthermore, to reduce the edge effects,the noisy data can be previously completed with zeros or using a mirror effect on its edges.

According to the sliding sub-window processing, only the sample located in the middle of the window is estimated, so that relation (56) becomes:

$$\widetilde{S}_{Q[k]}[k] = \sum_{m=1}^{Q[k]} z_{m,k} \Psi_m \left[\frac{K+1}{2}\right], \tag{68}$$

with:

$$z_{m,k} = \mathbf{Z_k}^T \mathbf{\Phi_m} \tag{69}$$

and where $Q[k]$ corresponds to the number of eigenvalues λ_m times the signal to noise ratio of window $\mathbf{Z_k}$ greater than one, i.e.:

$$\lambda_m \left.\frac{S}{N}\right|_{\mathbf{Z_k}} > 1. \tag{70}$$

To estimate the signal to noise ratio of window $\mathbf{Z_k}$, the signal power is directly computed from the window's data and the noise power is estimated on a part of the noisy data $\mathbf{Z}$, where no useful signal *a priori* occurs. This estimation is generally realized using the maximum likelihood principle.
Using relations (68) and (69), the estimation of the de-noised sample value is realized by a scalar product:

$$\widetilde{S}_{Q[k]}[k] = \mathbf{Z_k}^T \sum_{m=1}^{Q[k]} \Psi_m \left[\frac{K+1}{2}\right] \mathbf{\Phi_m}. \tag{71}$$

In this case and taking into account the sub-window size, reduced covariances $\mathbf{\Gamma_{S_0S_0}}$ and $\mathbf{\Gamma_{N_0N_0}}$ are both $K \times K$ matrices, so that $\{\mathbf{\Phi_n}\}$ and $\{\mathbf{\Psi_n}\}$ are K-dimensional basis.
Such an approach can be completed using the following relation:

$$\widetilde{S}_{Q[k]}[k] = \mathbf{Z_k}^T \mathbf{h_{Q[k]}}, \tag{72}$$

for k taking values between 1 and M, and where:

$$\mathbf{h_{Q[k]}} = \sum_{m=1}^{Q[k]} \Psi_m \left[\frac{K+1}{2}\right] \mathbf{\Phi_m}. \tag{73}$$

$Q[k]$ taking values between 1 and K, relation (73) permits to compute K vectors $\mathbf{h_q}$, from $\mathbf{h_1}$ ensuring a maximization of the signal to noise ratio, to $\mathbf{h_K}$ whose bandwidth corresponds to the whole useful signal bandwidth. These filters are called the stochastic matched filters for the following.

4.2.4 Algorithm

The algorithm leading to an approximation $\widetilde{\mathbf{S}}_\mathbf{Q}$ of the signal of interest $\mathbf{S}$, by the way of the stochastic extension of the matched filter, using a sliding sub-window processing, is presented below.

1. Modelisation or estimation of reduced covariances $\mathbf{\Gamma_{S_0S_0}}$ and $\mathbf{\Gamma_{N_0N_0}}$ of signal of interest and noise respectively.
2. Estimation of the noise power σ_N^2 in an homogeneous area of $\mathbf{Z}$.
3. Determination of eigenvectors $\mathbf{\Phi_m}$ by solving the generalized eigenvalue problem described in (22) or (42).
4. Normalization of $\mathbf{\Phi_m}$ according to (34) or (43).
5. Determination of vectors $\mathbf{\Psi_n}$ (relation (35) or (44)).
6. Computation of the K stochastic matched filters $\mathbf{h_q}$ according to (73).
7. Set to zero M samples approximation $\widetilde{\mathbf{S}}_\mathbf{Q}$.
8. For $k = 1$ to M do:

(a) Sub-window $\mathbf{Z_k}$ extraction.

(b) $\mathbf{Z_k}$ signal to noise ratio estimation.

(c) $Q[k]$ determination according to (70).

(d) Scalar product (72) computation.

Let us note the adaptive nature of this algorithm, each sample being processed with the most adequate filter $\mathbf{h_q}$ depending on the native signal to noise ratio of the processed sub-window.

4.3 Experiments

In this section, we propose two examples of de-noising on synthetic and real data in the case of 2-D discrete-space signals.

4.3.1 2-D discrete-space simulated data

As a first example, consider the Lena image presented in figure 1. This is a 512×512 pixels coded with 8 bits (i.e. 256 gray levels). This image has been artificially noise-corrupted by a zero-mean, Gaussian noise, where the local variance of the noise is a function of the image intensity values (see figure 3.a).

Fig. 1. Lena image, 512×512 pixels, 8 bits encoded (256 gray levels)

The stochastic matched filtering method is based on the assumption of signal and noise stationarity. Generally it is the case for the noise. However, the signal of interest is not necessarily stationary. Obviously, some images can be empirically supposed stationary, it is the case for sea-bed images, for some ocean waves images, in other words for all images able to be assimilated to a texture. But in most cases, an image cannot be considered as the realization of a stationary stochastic process. However after a segmentation operation, it is possible to define textured zones. This way, a particular zone of an image (also called window) can be considered as the realization of a stationary bi-dimensional stochastic process. The dimensions of these windows must be of the same order of magnitude as the texture coherence length. Thus, the stochastic matched filter will be applied on the native image using a windowed processing. The choice of the window dimensions is conditioned by the texture coherence length

mean value.
The implementation of the stochastic matched filter needs to have an *a priori* knowledge of signal of interest and noise covariances. The noise covariance is numerically determined in an homogeneous area of the observation, it means in a zone without any *a priori* information on signal of interest. This covariance is computed by averaging several realizations. The estimated power spectral density associated to the noise covariance is presented on figure 2.a. The signal of interest covariance is modeled analytically in order to match the different textures of the image. In dimension one, the signal of interest autocorrelation function is generally described by a triangular function because its associated power spectral density corresponds to signals with energy contained inside low frequency domain. This is often the case in reality. The model used here is a bi-dimensional extension of the mono-dimensional case. Furthermore, in order to not favor any particular direction of the texture, the model has isotropic property. Given these different remarks, the signal of interest autocorrelation function has been modeled using a Gaussian model, as follows:

$$\Gamma_{S_0S_0}[n,m] = \exp\left[-\left(n^2+m^2\right)/(2F_e^2\sigma^2)\right], \quad \forall (n,m) \in \mathbb{Z}^2, \tag{74}$$

with n and m taking values between $-(K-1)$ and $(K-1)$, where F_e represents the sampling frequency and where σ has to be chosen so as to obtain the most representative power spectral density. $\Gamma_{S_0S_0}$ being Gaussian, its power spectral density is Gaussian too, with a variance σ_ν^2 equal to $1/(4\pi^2\sigma^2)$. As for a Gaussian signal, 99 % of the signal magnitudes arise in the range $[-3\sigma_\nu;3\sigma_\nu]$, we have chosen σ_ν such as $6\sigma_\nu = F_e$, so that:

$$\sigma = 3/(\pi F_e). \tag{75}$$

The result power spectral density is presented on figure 2.b.

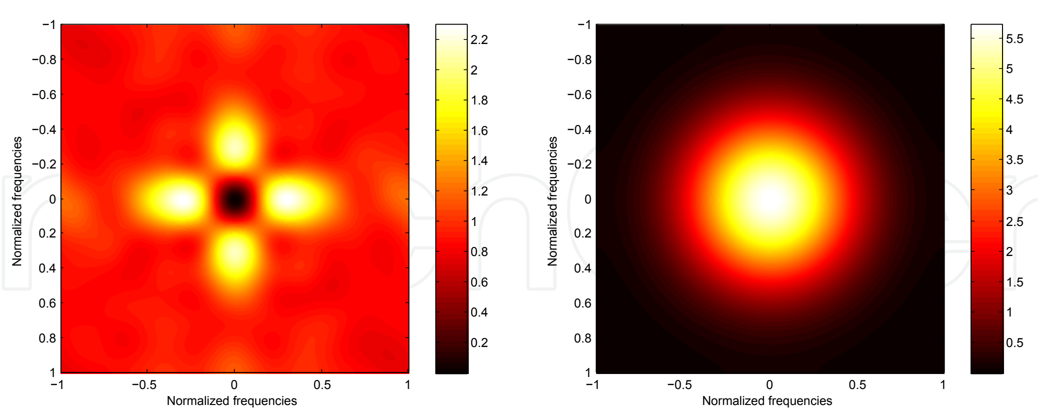

(a) Estimated noise PSD (b) Modeled signal PSD

Fig. 2. Signal and noise power spectral densities using normalized frequencies

The dimension of the filtering window for this process is equal to 7×7 pixels, in order to respect the average coherence length of the different textures. For each window, number Q of eigenvalues has been determined according to relation (70), with:

$$\left.\frac{S}{N}\right|_{\mathbf{Z_k}} = \frac{\sigma_{Z_k}^2 - \sigma_N^2}{\sigma_N^2}, \tag{76}$$

the noise variance σ_N^2 being previously estimated in an homogeneous area of the noise-corrupted data using a maximum likelihood estimator. The resulting image is presented on figure 3.b.

(a) Noisy Lena

(b) De-noised Lena

(c) Q values

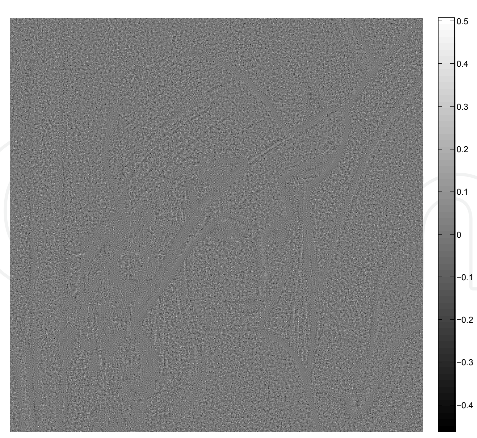

(d) Removed signal

Fig. 3. 1^{st} experiment: Lena image corrupted by a zero-mean Gaussian noise with a local variance dependent of the image intensity values

An analysis of the figure 3.b shows that the stochastic matched filter used as a de-noising process gives some good results in terms of noise rejection and detail preservation. In order to quantify the effectiveness of the process, we propose on figure 3.d an image of the removed signal $\widetilde{\mathbf{N}}$ (i.e. $\widetilde{\mathbf{N}} = \mathbf{Z} - \widetilde{\mathbf{S}}_{\mathbf{Q}}$), where the areas corresponding to useful signal details present an amplitude tending toward zero, the process being similar to an all-pass filter in order to preserve the spatial resolution. Nevertheless, the resulting image is still slightly noise-corrupted locally. It is possible to enhance the de-noising power increasing either the σ value (that corresponds to a diminution of the σ_v value and so to a smaller signal bandwidth) or the sub-image size, but this would involve a useful signal deterioration by a smoothing effect. In addition, the choice of the number Q of basis vectors by minimizing the mean square error between the signal of interest $\mathbf{S}$ and its approximation $\widetilde{\mathbf{S}}_{\mathbf{Q}}$ implies an image contour well preserved. As an example, we present in figures 3.c and 4 an image of the values of Q used for each window and a curve representative of the theoretical and real improvement of the signal to noise ratio according to these values (relation (66)).

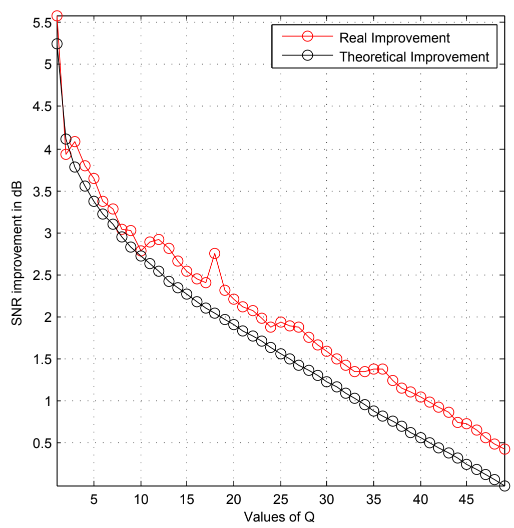

Fig. 4. Theoretical and real SNR improvement in dB of the de-noised data

As previously specified, when the signal to noise ratio is favorable a lot of basis vectors are retained for the filtering. In this case, the stochastic matched filter tends to be an all-pass filter, so that the signal to noise ratio improvement is not significant. On the other hand, when the signal to noise ratio is unfavorable this filtering method allows a great improvement (up to $5\,dB$ when only from 1 up to 2 basis vectors were retained), the stochastic matched filter being similar to a mean filter. Furthermore, the fact that the curves of the theoretical and real improvements are similar reveals the relevance of the signal covariance model.

4.3.2 2-D discrete-space real data

The second example concerns real 2-D discrete-space data acquired by a SAS (Synthetic Aperture Sonar) system. Over the past few years, SAS has been used in sea bed imagery. Active synthetic aperture sonar is a high-resolution acoustic imaging technique that coherently combines the returns from multiple pings to synthesize a large acoustic aperture. Thus, the azimuth resolution of a SAS system does not depend anymore on the length of

the real antenna but on the length of the synthetic antenna. Consequently, in artificially removing the link between azimuth resolution and physical length of the array, it is now possible to use lower frequencies to image the sea bed and keep a good resolution. Therefore, lower frequencies are less attenuated and long ranges can be reached. All these advantages make SAS images of great interest, especially for the detection, localization and eventually classification of objects lying on the sea bottom. But, as any image obtained with a coherent system, SAS images are corrupted by the speckle noise. Such a noise gives a granular aspect to the images, by giving a variance to the intensity of each pixel. This reduces spatial and radiometric resolutions. This noise can be very disturbing for the interpretation and the automatic analysis of SAS images. For this reason a large amount of research works have been dedicated recently to reduce this noise, with as common objectives the strong reduction of the speckle level, coupled to the spatial resolution preservation.
Consider the SAS image[1] presented in figure 5.a. This is a 642×856 pixels image of a wooden barge near Prudence Island. This barge measures roughly 30 meters long and lies in 18 meters of water.

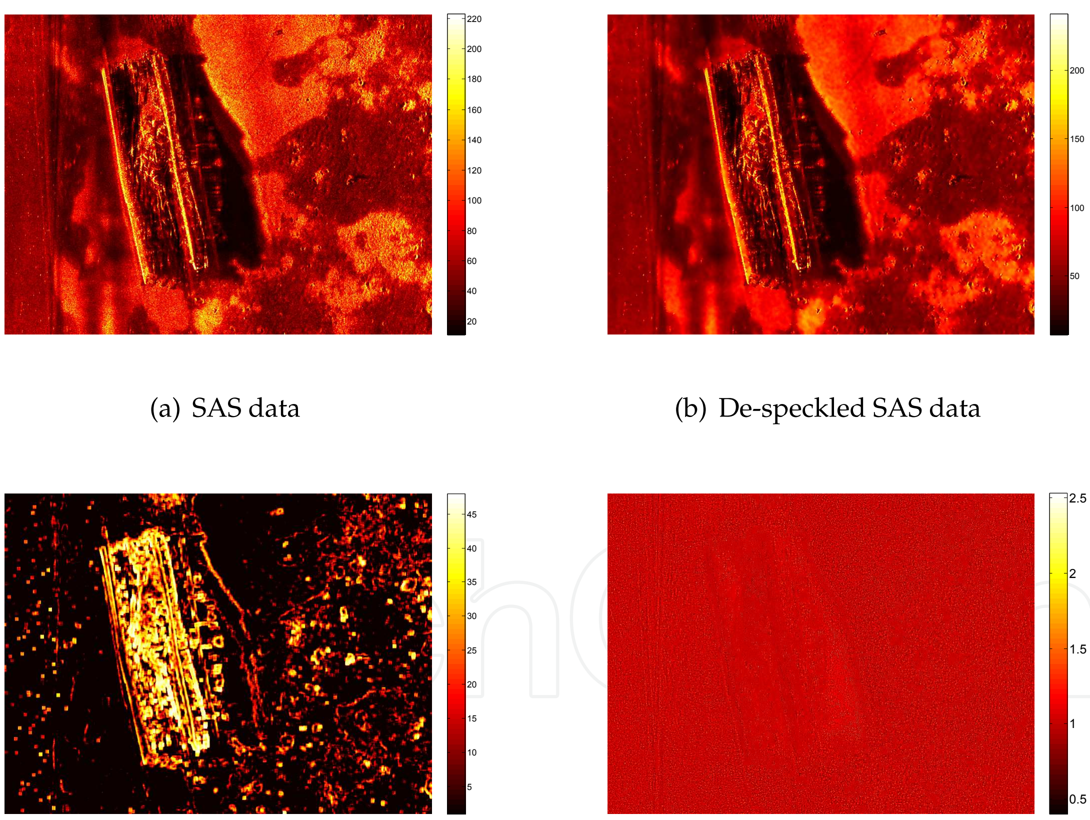

(a) SAS data (b) De-speckled SAS data

(c) Q values (d) Removed signal

Fig. 5. 2^{nd} experiment: Speckle noise corrupted SAS data: Wooden Barge (Image courtesy of AUVfest 2008)

[1] Courtesy of AUVfest 2008: *http://oceanexplorer.noaa.gov*

The same process than for the previous example has been applied to this image to reduce the speckle level. The main differences between the two experiments rest on the computation of the signal and noise statistics. As the speckle noise is a multiplicative noise (see relation (48)), the noise covariance, the noise power and the noise mean value have been estimated on the high-frequency components $\mathbf{Z_{h_{HF}}}$ of an homogeneous area $\mathbf{Z_h}$ of the SAS data:

$$\mathbf{Z_{h_{HF}}} = \mathbf{Z_h}./\mathbf{Z_{h_{BF}}}, \tag{77}$$

where ./ denotes the term by term division and with $\mathbf{Z_{h_{BF}}}$ corresponding to the low-frequency components of the studied area obtained applying a classical low-pass filter. This way, all the low-frequency fluctuations linked to the useful signal are canceled out.
Furthermore, taking into account the multiplicative nature of the noise, to estimate the signal to noise ratio $\left.\frac{S}{N}\right|_{\mathbf{Z_k}}$ of the studied window, the signal variance has been computed as follows:

$$\sigma_{S_k}^2 = \frac{\sigma_{Z_k}^2 + E\left\{\mathbf{Z_k}\right\}^2}{\sigma_N^2 + \bar{N}^2} - E\left\{\mathbf{S_k}\right\}, \tag{78}$$

where:

$$E\left\{\mathbf{S_k}\right\} = \frac{E\left\{\mathbf{Z_k}\right\}^2}{\bar{N}^2}. \tag{79}$$

The de-noised SAS data is presented on figure 5.b. An image of the Q values retained for the process and the ratio image $\mathbf{Z}./\widetilde{\mathbf{S}}_{\mathbf{Q}}$ are proposed on figures 5.c and 5.d respectively. These results show that the stochastic matched filter yields good speckle noise reduction, while keeping all the details with no smoothing effect on them (an higher number of basis vectors being retained to process them), so that the spatial resolution seems not to be affected.

4.4 Concluding remarks

In this section, we have presented the stochastic matched filter in a de-noising context. This one is based on a truncation to order Q of the random noisy data expansion (56). To determine this number Q, it has been proposed to minimize the mean square error between the signal of interest and its approximation. Experimental results have shown the usefulness of such an approach. This criterion is not the only one, one can apply to obtain Q. The best method to determine this truncature order may actually depend on the nature of the considered problem. For examples, the determination of Q has been achieved in (Fraschini et al., 2005) considering the Cramér-Rao lower bound and in (Courmontagne, 2007) by the way of a minimization between the speckle noise local statistics and the removal signal local statistics. Furthermore, several stochastic matched filter based de-noising methods exist in the scientific literature, as an example, let cite (Courmontagne & Chaillan, 2006), where the de-noising is achieved using several signal covariance models and several sub-image sizes depending on the windowed noisy data statistics.

5. The Stochastic Matched Filter in a detection context

In this section, the stochastic matched filter is described for its application in the field of short signal detection in a noisy environment.

5.1 Problem formulation

Let consider two hypotheses $\mathcal{H}_0$ and $\mathcal{H}_1$ corresponding to "*there is only noise in the available data*" and "*there is signal of interest in the available data*" respectively and let consider a K-dimensional vector $\mathbf{Z}$ containing the available data. The dimension K is assumed large (i.e. $K >> 100$). Under hypothesis $\mathcal{H}_0$, $\mathbf{Z}$ corresponds to noise only and under hypothesis $\mathcal{H}_1$ to a signal of interest $\mathbf{S}$ corrupted by an additive noise $\mathbf{N}$:

$$\begin{cases} \mathcal{H}_0 & : \quad \mathbf{Z} = \sigma_N \mathbf{N_0} \\ \mathcal{H}_1 & : \quad \mathbf{Z} = \sigma_S \mathbf{S_0} + \sigma_N \mathbf{N_0} \end{cases}, \tag{80}$$

where σ_S and σ_N are signal and noise standard deviation respectively and $E\left\{|\mathbf{S_0}|^2\right\} = E\left\{|\mathbf{N_0}|^2\right\} = 1$. By assumptions, $\mathbf{S_0}$ and $\mathbf{N_0}$ are extracted from two independent, stationary and zero-mean random signals of known autocorrelation functions. This allows us to construct the covariances of $\mathbf{S_0}$ and $\mathbf{N_0}$ denoted $\mathbf{\Gamma_{S_0S_0}}$ and $\mathbf{\Gamma_{N_0N_0}}$ respectively.
Using the stochastic matched filter theory, it is possible to access to the set $(\mathbf{\Phi_m}, \lambda_m)_{m=1\ldots M}$, with M bounded by K, allowing to compute the uncorrelated random variables z_m associated to observation $\mathbf{Z}$. It comes:

$$\begin{cases} E\left\{z_m^2/\mathcal{H}_0\right\} = \sigma_N^2 \\ E\left\{z_m^2/\mathcal{H}_1\right\} = \sigma_S^2\lambda_m + \sigma_N^2 \end{cases}. \tag{81}$$

Random variables z_m being a linear transformation of a random vector, the central limit theorem can be invoked and we will assume in the sequel that z_m are approximately Gaussian:

$$z_m \hookrightarrow \mathcal{N}\left(0, E\left\{z_m^2/\mathcal{H}_i\right\}\Big|_{i=0,1}\right). \tag{82}$$

Let $\mathbf{\Gamma_0}$ and $\mathbf{\Gamma_1}$ be the covariances of the signals in the basis $\{\mathbf{\Phi_m}\}_{m=1\ldots M}$, under hypotheses $\mathcal{H}_0$ and $\mathcal{H}_1$, it comes:

$$\mathbf{\Gamma_0} = \sigma_N^2 \mathbf{I}, \tag{83}$$

where $\mathbf{I}$ denotes the $M \times M$ identity matrix and

$$\mathbf{\Gamma_1} = \begin{pmatrix} \sigma_S^2\lambda_1 + \sigma_N^2 & 0 & 0 & \ldots & 0 \\ 0 & \sigma_S^2\lambda_2 + \sigma_N^2 & 0 & \ldots & 0 \\ \vdots & \ddots & \ddots & \ddots & \vdots \\ 0 & \ldots & \ldots & 0 & \sigma_S^2\lambda_M + \sigma_N^2 \end{pmatrix}. \tag{84}$$

In these conditions, the probability density functions under hypotheses $\mathcal{H}_0$ and $\mathcal{H}_1$ take for expression:

$$\begin{cases} p(\mathbf{z}/\mathcal{H}_0) = \dfrac{1}{(2\pi)^{\frac{M}{2}}\sqrt{|\mathbf{\Gamma_0}|}} \exp\left[\dfrac{-1}{2}\left(\mathbf{z}^T\mathbf{\Gamma_0}^{-1}\mathbf{z}\right)\right] \\ p(\mathbf{z}/\mathcal{H}_1) = \dfrac{1}{(2\pi)^{\frac{M}{2}}\sqrt{|\mathbf{\Gamma_1}|}} \exp\left[\dfrac{-1}{2}\left(\mathbf{z}^T\mathbf{\Gamma_1}^{-1}\mathbf{z}\right)\right] \end{cases}, \tag{85}$$

where $\mathbf{z}$ is a $M-$dimensional vector, whose m^{th} component is z_m:

$$\mathbf{z} = (z_1, z_2, \ldots, z_m, \ldots, z_M)^T. \tag{86}$$

It is well known that the Neyman-Pearson lemma yields the uniformly most powerful test and allows to obtain the following rule of decision based on the likelihood ratio $\Lambda(\mathbf{z})$:

$$\Lambda(\mathbf{z}) = \frac{p(\mathbf{z}/\mathcal{H}_1)}{p(\mathbf{z}/\mathcal{H}_0)} \underset{D_0}{\overset{D_1}{\gtrless}} \lambda, \tag{87}$$

where λ is the convenient threshold.
Taking into account relations (83), (84) and (85), it comes:

$$\underbrace{\sum_{m=1}^{M} \frac{\lambda_m}{\sigma_S^2 \lambda_m + \sigma_N^2}}_{U_M} \gtrless_{D_0}^{D_1} \underbrace{\frac{\sigma_N^2}{\sigma_S^2} \left[2\left(\ln \lambda - M \ln \sigma_N\right) + \sum_{m=1}^{M} \ln\left(\sigma_S^2 \lambda_m + \sigma_N^2\right) \right]}_{T_M}. \tag{88}$$

In these conditions, the detection and the false alarm probabilities are equal to:

$$P_d = \int_{T_M}^{\infty} p_{U_M}(u/\mathcal{H}_1) du \quad \text{and} \quad P_{fa} = \int_{T_M}^{\infty} p_{U_M}(u/\mathcal{H}_0) du. \tag{89}$$

So, the detection problem consists in comparing u to threshold T_M and in finding the most convenient order M for an optimal detection (i.e. a slight false alarm probability and a detection probability quite near one).

5.2 Subspace of dimension one

First, let consider the particular case of a basis $\{\mathbf{\Phi_m}\}_{m=1\ldots M}$ restricted to only one vector $\mathbf{\Phi}$. In this context, relation (88) leads to:

$$|z| \gtrless_{D_0}^{D_1} \underbrace{\sqrt{\frac{T_1}{\lambda_1}(\sigma_S^2 \lambda_1 + \sigma_N^2)}}_{z_s} \tag{90}$$

and the detection and false alarm probabilities become:

$$P_d = \int_{D_1} p(z/\mathcal{H}_1) dz \quad \text{and} \quad P_{fa} = \int_{D_1} p(z/\mathcal{H}_0) dz, \tag{91}$$

where $D_1 =]-\infty; -z_s] \cup [z_s; +\infty[$ and with:

$$\begin{cases} \text{under } \mathcal{H}_0 : z \hookrightarrow \mathcal{N}\left(0, \sigma_N^2\right) \\ \text{under } \mathcal{H}_1 : z \hookrightarrow \mathcal{N}\left(0, \sigma_S^2 \lambda_1 + \sigma_N^2\right) \end{cases}. \tag{92}$$

From (91), it comes:

$$P_{fa} = 1 - \text{erf}\left(\frac{z_s}{\sqrt{2}\sigma_N}\right), \tag{93}$$

where erf(.) denotes the error function:

$$\text{erf}(x) = \frac{2}{\sqrt{\pi}} \int_0^x \exp\left[-y^2\right] dy. \tag{94}$$

In these conditions, the threshold value z_s can be expressed as a function of the false alarm probability:

$$z_s = \sqrt{2}\sigma_N \text{erf}^{-1}(1 - P_{fa}). \tag{95}$$

Furthermore, the detection probability takes the following expression:

$$P_d = 1 - \mathrm{erf}\left(\frac{z_s}{\sqrt{2\left(\sigma_S^2\lambda_1 + \sigma_N^2\right)}}\right). \tag{96}$$

We deduce from equations (95) and (96), the ROC curve expression:

$$P_d\left(P_{fa}\right) = 1 - \mathrm{erf}\left(\sqrt{\frac{1}{1+\rho_0\lambda_1}}\mathrm{erf}^{-1}(1-P_{fa})\right), \tag{97}$$

where $\rho_0 = \sigma_S^2/\sigma_N^2$.
One can show that an optimal detection is realized, when λ_1 corresponds to the greatest eigenvalue of the generalized eigenvalue problem (22).

5.3 Subspace of dimension M

Random variable U_M being a weighted sum of square Gaussian random variables, its probability density function, under hypotheses $\mathcal{H}_0$ and $\mathcal{H}_1$, can be approximated by a Gamma law (Kendall & Stuart, 1979; Zhang & Liu, 2002). It comes:

$$p_{U_M}(u/\mathcal{H}_i) \simeq u^{k_i-1}\frac{\exp\left[\frac{-u}{\theta_i}\right]}{\Gamma(k_i)\theta_i^{k_i}}, \tag{98}$$

for i equal 0 or 1 and where $k_0\theta_0 = E\{U_M/\mathcal{H}_0\}$, $k_0\theta_0^2 = \mathrm{VAR}\{U_M/\mathcal{H}_0\}$, $k_1\theta_1 = E\{U_M/\mathcal{H}_1\}$ and $k_1\theta_1^2 = \mathrm{VAR}\{U_M/\mathcal{H}_1\}$. In these conditions, it comes under $\mathcal{H}_0$:

$$k_0 = \frac{\left(\sum_{m=1}^{M}\frac{\lambda_m}{1+\rho_0\lambda_m}\right)^2}{2\sum_{m=1}^{M}\left(\frac{\lambda_m}{1+\rho_0\lambda_m}\right)^2} \quad \text{and} \quad \theta_0 = 2\frac{\sum_{m=1}^{M}\left(\frac{\lambda_m}{1+\rho_0\lambda_m}\right)^2}{\sum_{m=1}^{M}\frac{\lambda_m}{1+\rho_0\lambda_m}} \tag{99}$$

and, under $\mathcal{H}_1$:

$$k_1 = \frac{\left(\sum_{m=1}^{M}\lambda_m\right)^2}{2\sum_{m=1}^{M}\lambda_m^2} \quad \text{and} \quad \theta_1 = 2\frac{\sum_{m=1}^{M}\lambda_m^2}{\sum_{m=1}^{M}\lambda_m}. \tag{100}$$

It has been shown in (Courmontagne et al., 2007) that the use of the stochastic matched filter basis $\{\mathbf{\Phi_m}\}_{m=1\ldots M}$ ensures a maximization of the distance between the maxima of $p_{U_M}(u/\mathcal{H}_0)$ and $p_{U_M}(u/\mathcal{H}_1)$ and so leads to an optimal detection.
The basis dimension M is determined by a numerical way. As the detection algorithm is applied using a sliding sub-window processing, each sub-window containing K samples, we can access to K eigenvectors solution of the generalized eigenvalue problem (22). For each

value of M, bounded by 2 and K, we numerically determine the threshold value T_M allowing a wanted false alarm probability and according to the following relation:

$$P_{fa} = 1 - \Delta u^{k_0} \sum_{q=0}^{Q_M} q^{k_0 - 1} \frac{\exp\left[\frac{-q\Delta u}{\theta_0}\right]}{\Gamma(k_0)\theta_0^{k_0}}, \tag{101}$$

where $T_M = Q_M \Delta u$.
Then for each value of T_M, we compute the detection probability according to:

$$P_d = 1 - \Delta u^{k_1} \sum_{q=0}^{Q_M} q^{k_1 - 1} \frac{\exp\left[\frac{-q\Delta u}{\theta_1}\right]}{\Gamma(k_1)\theta_1^{k_1}}. \tag{102}$$

Finally, the basis dimension will correspond to the M value leading to a threshold value T_M allowing the highest detection probability.

5.4 Experiments

5.4.1 Whale echoes detection

Detecting useful information in the underwater domain has taken an important place in many research works. Whether it is for biological or economical reasons it is important to be able to correctly distinguish the many kinds of entities which belong to animal domain or artificial object domain.
For this reason, we have chosen to confront the proposed process with signals resulting from underwater acoustics. The signal of interest **S** corresponds to an acoustic record of several whale echoes. The sampling rate used for this signal is 44100 Hz. Each echo lasts approximatively two seconds. The disturbing signal **N** corresponds to a superposition of various marine acoustic signatures. The simulated received noisy signal **Z** has been constructed as follows:

$$\mathbf{Z} = \mathbf{S} + g\mathbf{N}, \tag{103}$$

where g is a SNR control parameter allowing to evaluate the robustness of the detection processing. Several realizations were built with a SNR taking values from $-12\,dB$ to $12\,dB$ (the SNR corresponds to the ratio of the signal and noise powers in the common spectral bandwidth). As an example, we present on figure 7.a in black lines the noisy data in the case of a SNR equal to $-6\,dB$. On the same graph, in red lines, we have reported the useful signal **S**.
The signal and noise covariances were estimated on signals belonging to the same series of measurement as the signal **S** and the noise **N**. The signal covariance was obtained by fitting a general model based on the average of several realizations of whale clicks while the noise one was estimated from a supposed homogeneous subset of the record.
The ROC curves numerically obtained by the way of relations (101) and (102) with the probability density functions described by relations (98) are presented on figure 6 (for a signal to noise ratio greater than $-8\,dB$ the ROC curves are practically on the graph axes). There are 512 samples in the sub-window, so we can access to 512 eigenvectors (i.e. 512 is the maximal size of the basis). Basis dimension M takes values between 17 and 109 depending on the studied signal to noise ratio ($M = 17$ for $\left.\frac{S}{N}\right|_{\mathbf{Z}} = 12\,dB$ and $M = 109$ for $\left.\frac{S}{N}\right|_{\mathbf{Z}} = -12\,dB$).

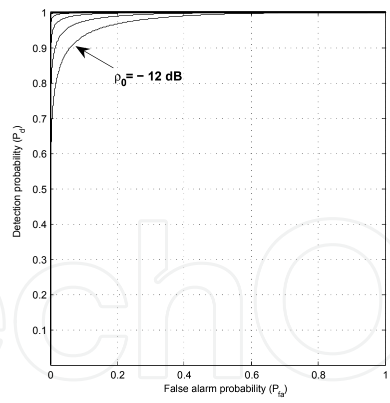

Fig. 6. ROC curves for a SNR taking values in $[-12\,dB; 12\,dB]$

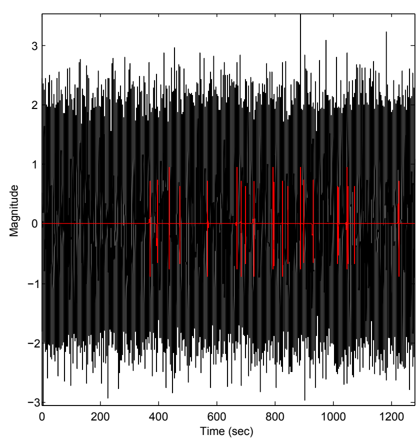

(a) Noisy data with a SNR equal to $-6\,dB$

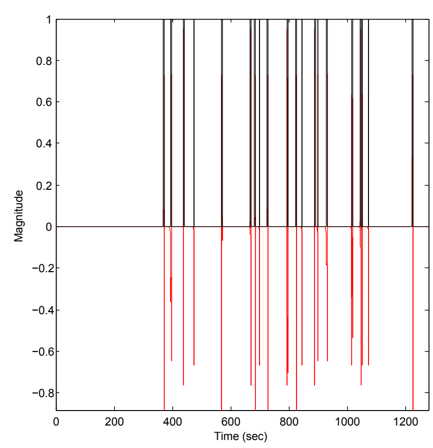

(b) Result of the detection algorithm

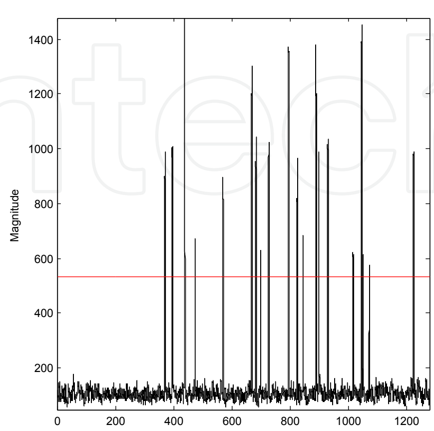

(c) U_M and T_M according to (88)

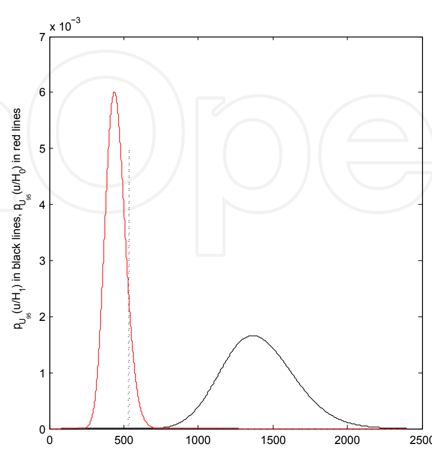

(d) Probability density functions $p_{U_M}(u/\mathcal{H}_0)$ and $p_{U_M}(u/\mathcal{H}_1)$

Fig. 7. 1^{st} experiment: Whale echoes detection

The false alarm probability has been settled to 10 %. The result to the detection process is proposed on figure 7.b in black lines. On the same graph, the useful signal has been reported in red lines, in order to verify that a detected event coincides with a whale echo. Figure 7.c presents the vector U_M and the automatic threshold T_M: the use of the stochastic matched filter allows to amplify the parts of the noisy data corresponding to whale echoes, while the noise is clearly rejected. As explained in a previous section, the efficiency of the stochastic matched filter is due to its property to dissociate the probability density functions, as shown in figure 7.d (on this graph appears in dashed lines the position of the threshold T_M for a $P_{fa} = 10\%$)).

5.4.2 Mine detection on SAS images

Detection and classification of underwater mines (completely or partially buried) with SAS images is a major challenge to the mine countermeasures community. In this context, experts are looking for more and more efficient detection processes in order to help them in their decisions concerning the use of divers, mines destruction ... As a mine highlight region usually has a corresponding shadow region (see figure 8), most of the methods used to detect and classify objects lying on the seafloor are based on the interpretation of the shadows of the objects. Other methods are focusing on the echo itself. For these approaches, two main problems could occur:

- given the position of the sonar fish and the type of mine encountered, the shape of the echo and its associated shadow zone could vary; but as most of these techniques of detection generally required training, their success can be dependent on the similarity between the training and test data sets,
- given that SAS images are speckle noise corrupted, it is generally necessary to denoise these images before of all; but such a despeckling step could involve miss and/or false detection by an alteration of the echo and/or shadow, given that most of the despeckling methods induce a smoothing effect.

In answer to these problems, we propose to use a one-dimensional detector based on the stochastic matched filter. This detector is applied on each line of the SAS data (considering as a line the data vector in a direction perpendicular to the fish direction). In this context, we construct a very simple model of the signal to be detected (see figure 8), where d, the size of the echo in sight, is a uniform random variable taking values in a range dependent of the mine dimensions. So the problem of mine detection in SAS images is reduced to the one of detecting a one-dimensional signal, such as the model presented in figure 8, in a noisy data vector $\mathbf{Z}$.

As the length of the shadow region depends on the fish height, we do not consider the whole shadow for our model, but only its beginning (this corresponds to the length D in figure 8).

The signal covariance is estimated using several realizations of the signal model by making varied the random variable d value. For the noise, its covariance is computed in an area of the data, where no echo is assumed to be present and takes into account the hilly seabed.

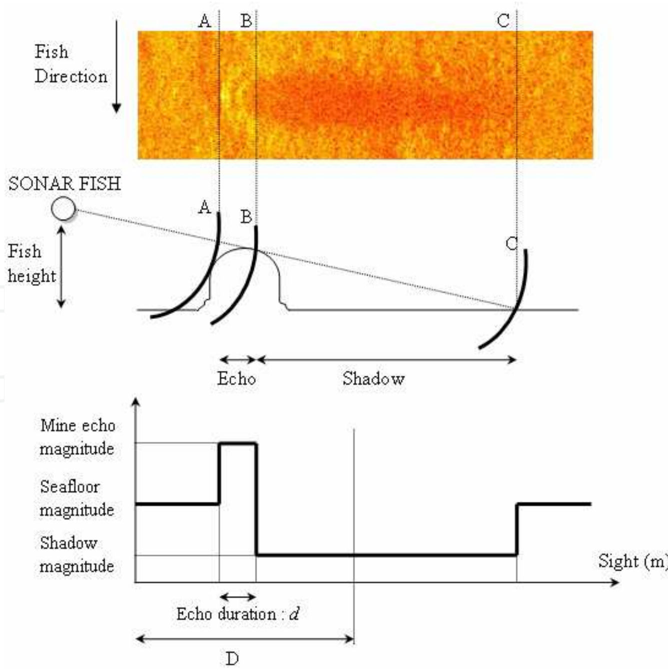

Fig. 8. Signal model: the wave is blocked by objects lying on seafloor and a shadow is generated

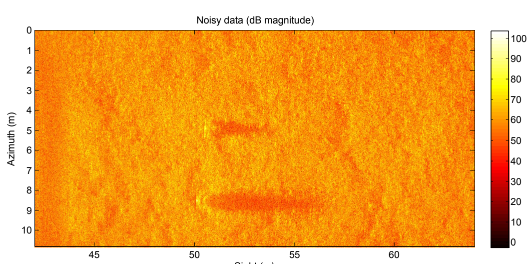

(a) SAS image representing a sphere and a more complex mine like object lying on the seafloor

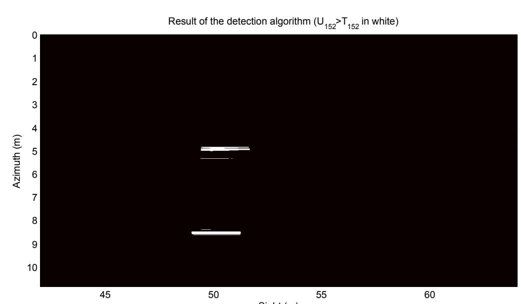

(b) Result of the detection algorithm

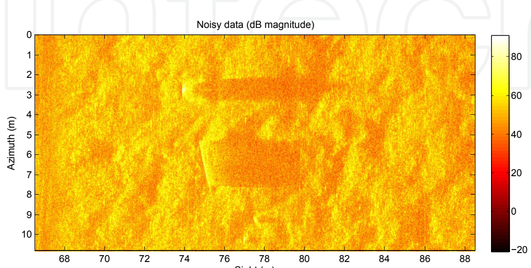

(c) SAS image representing two mine like objects: a sphere and a cylinder lying on its side

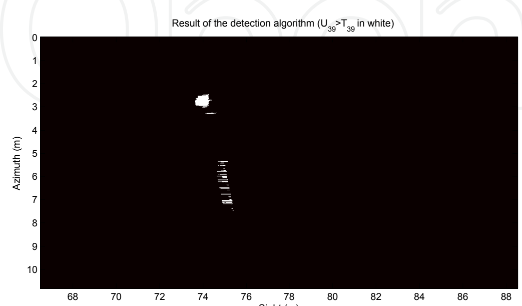

(d) Result of the detection algorithm

Fig. 9. 2^{nd} experiment: Mine detection on SAS images

The data set used for this study has been recorded in 1999 during a joint experiment between GESMA (Groupe d'Etudes Sous-Marines de l'Atlantique, France) and DERA (Defence Evaluation and Research Agency, United Kingdom). The sonar was moving along a fixed rail and used a central frequency of $150\,kHz$ with a bandwidth of $64\,kHz$. Figure 9.a and 9.c present two images obtained during this experiment[2]. We recognize the echoes (the bright pixels) in front of the objects and the shadows behind as well as the speckle that gives the granular aspect to the image. Because of the dynamics of the echo compared to the remainder of the image, these figures are represented in dB magnitude.
As the dimensions of the two mine like objects in azimuth and sight are not greater than one meter, the proposed process has been calibrated to detect objects which dimensions in sight are included in the range $[0.5\,m; 1\,m]$ (i.e. the uniform random variable from the signal model takes values in $[0.5; 1]$). For these two experiments, the false alarm probability has been settled to 0.1%, entailing a basis dimension M equal to 152 for the first one and to 39 for the second one. The results obtained applying the detection algorithm are presented on figures 9.b and 9.d. For the two cases, the mine like objects are well detected, without false alarm. These results demonstrate the advantages of such a detection scheme, even in difficult situations, such as the one presented on figure 9.c.

6. Conclusions

This chapter concerned the problem of a noise-corrupted signal expansion and its applications to detection and signal enhancement. The random signal expansion, used here, is the stochastic matched filtering technique. Such a filtering approach is based on the noisy data projection onto a basis of known vectors, with uncorrelated random variables as decomposition coefficients. The basis vectors are chosen such as to maximize the signal to noise ratio after denoising. Several experiments in the fields of short signal detection in a noisy environment and of signals de-noising have shown the efficiency of the proposed expansion, even for unfavorable signal to noise ratio.

7. References

K. Karhunen, Zur spektraltheorie stochastischer prozesse, *Ann. Acad. Sci. Fennicae*, *N^o* 37, 1946, pp. 1-37.

M.M. Loève, *Probability theory*, Princeton, N.J. : Van Nostrand, 1955.

J.-F. Cavassilas, Stochastic matched filter, *Proceedings of the Institute of Acoustics (International Conference on Sonar Signal Processing)*, pp. 194-199, Vol. 13, Part 9, 1991.

F. Chaillan, C. Fraschini and P. Courmontagne, Speckle Noise Reduction in SAS Imagery, *Signal Processing*, Vol. 87, *N^o* 4, 2007, pp. 762-781.

F. Chaillan, C. Fraschini and P. Courmontagne, Stochastic Matched Filtering Method Applied to SAS Imagery, *Proceedings of OCEANS'05*, pp. 233-238, Vol. 1, June 2005, Brest, France.

M. Tur, K.C. Chin, J.W. Goodman, When is speckle noise multiplicative?, *Applied optics*, Vol.21, *N^o* 7, 1982, pp.1157-1159.

D. T. Kuan, A. A. Sawchuk, T. C. Strand and P. Chavel, Adaptative noise smoothing filter for images with signal-dependent noise, *IEEE Transactions on Pattern Analysis and Machine Intelligence*, Vol. 7, *N^o* 2, 1985, pp. 165-177.

H. L. Vann Trees, *Detection, Estimation, and Modulation Theory, Part I.*, Wiley, New York, 1968.

[2] Courtesy of GESMA, France

C. Fraschini, F. Chaillan and P. Courmontagne, An improvement of the discriminating capability of the active SONAR by optimization of a criterion based on the Cramer-Rao lower bound, *Proceedings of OCEANS'05*, pp. 804-809, Vol. 2, June 2005, Brest, France.

P. Courmontagne, SAS Images De-noising: The Jointly Use of an Autoadaptive Mean Filter and the Stochastic Matched Filter, *Proceedings of OCEANS'07*, June 2007, Aberdeen, Scotland.

P. Courmontagne and F. Chaillan, The Adaptive Stochastic Matched Filter for SAS Images Denoising, *Proceedings of OCEANS'06*, September 2006, Boston, USA.

M. Kendall and A. Stuart, *The Advanced Theory of Statistics*, London: Charles Griffin, Vol. 2, 1979.

Q. Zhang and D. Liu, A simple capacity formula for correlated diversity Rician fading channels, *IEEE Communications Letters*, Vol. 6, N^o 11, 2002, pp. 481-483.

Ph. Courmontagne, N. Vergnes and C. Jauffret, An optimal subspace projection for signal detection in noisy environment, *Proceedings of OCEANS'07*, September 2007, Vancouver, Canada.

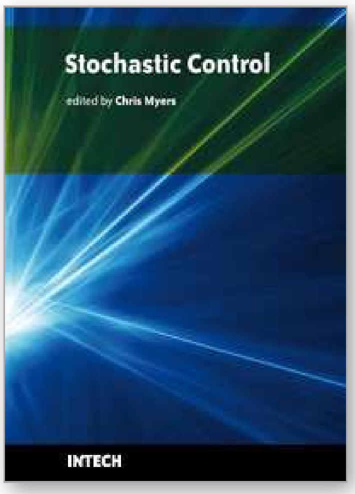

Stochastic Control
Edited by Chris Myers

ISBN 978-953-307-121-3
Hard cover, 650 pages
Publisher Sciyo
Published online 17, August, 2010
Published in print edition August, 2010

Uncertainty presents significant challenges in the reasoning about and controlling of complex dynamical systems. To address this challenge, numerous researchers are developing improved methods for stochastic analysis. This book presents a diverse collection of some of the latest research in this important area. In particular, this book gives an overview of some of the theoretical methods and tools for stochastic analysis, and it presents the applications of these methods to problems in systems theory, science, and economics.